The fish Strouhal number as a criterion for hydraulic fishway design

Link, O; Sanheuza, C; Arriagada, P; Brevis, W; Laborde, A; Gonzalez, A; Wilkes, M. and Habit, E.

Original citation:
Link, O; Sanheuza, C; Arriagada, P; Brevis, W; Laborde, A; Gonzalez, A; Wilkes, M. and Habit, E. (2017) The fish Strouhal number as a criterion for hydraulic fishway design. *Ecological Engineering* (103) Part A, June 2017, 118-126. DOI: 10.1016/j.ecoleng.2017.03.018

http://dx.doi.org/10.1016/j.ecoleng.2017.03.018

Elsevier

The fish Strouhal number as a criterion for hydraulic fishway design

Oscar Link[1,*] Claudia Sanhueza[1], Pedro Arriagada[1], Wernher Brevis[2], Anita Laborde[3], Alonso González[1], Martin Wilkes[4], Evelyn Habit[3]

[1]: Civil Engineering Department, Faculty of Engineering, and CRHIAM Center, Universidad de Concepción, Concepción, Chile

[2]: Civil Engineering Department, Faculty of Engineering, University of Sheffield, Sheffield, UK.

[3]: Department of Aquatic System, Faculty of Environmental Sciences, and EULA Centre, Universidad de Concepción, Concepción, Chile

[4]: Centre for Agroecology, Water and Resilience, Coventry University, Coventry, UK

*: corresponding author. Email: olink@udec.cl

Abstract

Longitudinal river fragmentation through physical barriers is a major issue for the conservation of aquatic species in regions with intense hydropower development, such as Chile. The construction of fishways is the main mitigation strategy for maintaining connectivity for fish but development of designs suitable for a broad range of species is challenging. Recent work has shown that two species native to Chile, *Cheirodon galusdae* and *Basilichthys microlepidotus* exhibited similar swimming performance in free flow in the laboratory, indicating that a single fishway design may be suitable for

both species. However, in the complex, three-dimensional altered flows observed in fishways, swimming performance is likely to vary from the free flow case due to the adoption of distinctive swimming gaits, variation in swimming styles, and the potentially destabilizing effects of wake vortices. In order to improve criteria for hydraulic design of fishways for multiple species we study the behavior and tail beat kinematics of *C. galusdae* and *B. microlepidotus* (juveniles), in the wake of vertical and bottom-mounted cylinders in an open channel flow. *Cheirodon galusdae* swam using a burst-and-coast style. This species avoided the cylinder wakes, searching for more favorable flow conditions. *Basilichthys microlepidotus* adopted a Kármán gait-like swimming strategy to swim in the cylinder wake. Tail beat frequency was constant in all experiments for both species, but in the presence of cylinders >2 cm in diameter, *C. galusdae* diminished the duration of the coast phase evidencing a higher propulsive effort. Tail beat amplitude of both species increased with the vortex length scale and decreased linearly with vortex shedding frequency. The fish Strouhal number correlated well with the relative vortex size and shedding frequency, compiling the swimming effort of species with very different behaviors, indicating that it is a suitable criterion for fishway design.

Keywords: Multispecies fishways; Design criteria; Fish behavior in wakes; Tail beat kinematics; Turbulence.

1. Introduction

The decline of freshwater fish biodiversity is occurring at an alarming and persistent rate (Butchart et al., 2010). Given that most fish must undertake some form of movement to complete their life cycle, the high proliferation of hydropower schemes is of particular concern since longitudinal river fragmentation through physical barriers is a major issue for the conservation of aquatic species. Moreover, impacts of hydropower facilities and other instream structures, such as weirs and culverts, which block fish movements are especially complex in regions with diverse and poorly understood fish stocks (Castro-Santos et al., 2009). Several locations in the southern hemisphere such as Brazil, Perú and Chile, are among the major global hotspots of hydropower development (Zarfl et al., 2015) and are home to some of the least studied ´non-sport´ fish communities in the world (Link and Habit, 2015).

Even when considered 'half-way' technologies (Brown et al., 2013) fishways, especially nature-like designs, are a promising alternative for provision of riverine connectivity to mitigate the critical impacts of barriers, such as longitudinal fragmentation (Baki et al., 2013; Baki et al., 2014). One of the greatest challenges in fish passage technology is the development of structures and design concepts suitable for a broad range of species (Castro-Santos et al., 2009; Russon and Kemp, 2011). The reasons explaining why some fishways work better than others and why some species perform better than others in particular fishways is still poorly understood. Some of the factors that affect fish passage in a fishway include: (1) biological characteristics as for instance the migration and movement patterns, body length, swimming and non-swimming (e.g. climbing) modes, circadian rhythms, and response to olfactory and acoustic stimuli; (2) ecological

characteristics, such as habitat and food preferences, light intensity and water temperature, and presence of conspecifics and predators; and (3) hydraulic properties of the fishway, including geometry, substrate and vegetation, length, slope, water depth, velocity and turbulence (Bunt et al., 2012; Noonan et al., 2012; Goettel et al., 2015; Link and Habit, 2015).

Of the aforementioned factors body length and hydraulics have received much attentions as, within a given species, fish swimming speed is proportional to body length (Videler & Wardle, 1991; Wardle et al., 1995; Stafkiotakis et al., 1999). This is especially important in the context of ensuring passage for non-sport fish that, by definition, are small-bodied (<150 mm total length at maturity) and have been described as having correspondingly weak swimming abilities in absolute terms (e.g. Mitchell 1989, Nikora et al., 2003; Plew et al., 2007). Laborde et al. (2016), however, have recently shown that two non-sport species native to Chile exhibit relatively strong swimming capacity during swimming tests in free flow in the laboratory. The swimming ability of the two species, *Cheirodon galusdae* and *Basilichthys microlepidotus*, under controlled conditions was similar, leading to the suggestion that an effective fishway could be designed to accommodate both species simultaneously. However, in the complex, three-dimensional altered flows observed in fishways (Feurich et al., 2012; Bretón et al., 2013; Baki et al., 2013; Baki et al., 2014) the swimming performance of fish is likely to vary from the free flow case due to the adoption of distinctive swimming gaits (Liao et al., 2003a; Liao et al., 2003b; Liao et al., 2007; Taguchi and Liao, 2011), variation in swimming styles (Weihs and Webb, 1983; Videler, 1993), and the potentially destabilizing effects of wake vortices (Pavlov et al., 2000; Lupandin, 2005; Tritico and Cotel, 2010). Depending on the intensity,

predictability (periodicity), orientation and scale of the turbulence relative to fish characteristics (e.g. body shape and length), swimming performance may be enhanced, diminished or unaffected in altered flows (Lacey et al., 2012; Wilkes et al., 2013; Enders and Boisclair, 2016).

An important aspect of swimming performance is related to propulsion through the caudal fin and thus, to tail beat kinematics, including tail beat frequency (f_{TB}) and amplitude (λ) in relation to swimming speed (U) (Bainbridge, 1958; Hunter and Zweifel, 1971; Videler and Wardle, 1991). Note that swimming speed would typically be equal to the flow velocity as, due to rheotaxis, the fish tends to hold position in the flow. In the following, U is the section averaged flow velocity. In particular, the fish Strouhal number, $St_{fish} = f_{TB}\,\lambda\,/\,U$, may be a useful dimensionless parameter for representing the propulsion effort of different fish species on a comparable basis. Extensive observations have shown that maximum propulsive efficiency lies in the range $0.25 < St_{fish} < 0.35$ for a large range of fish species (Triantafyllou et al., 1993; Eloy, 2012).

In this work, we study the behavior and tail beat kinematics of the native Chilean species, *C. galusdae* and *B. microlepidotus* (juveniles), in the wake of vertical and bottom-mounted cylinders in an open channel flow. The focus is on the variation in swimming styles, and the potentially destabilizing effects of wake vortices in order to improve criteria for hydraulic design of multispecific fishways, which urgently need to incorporate elements promoting the passage of small body sized fish. This research contributes to the conservation of non-sport fish species threatened due to pressures for hydropower development.

1. Methods

2.1. Studied species

Basilichthys microlepidotus inhabits the piedmont of the Andes and Central Valley from 21 to 40° latitude south (Véliz et al., 2012). Maximum body size is 120 mm for juveniles and 300 mm when adults. This species spawns and rears in floodplains during the austral spring (egg laying from November to December and larvae from November to February in the southern range of its distribution; Montoya et al., 2012). Diet varies from planktivorous to omnivorous and bentophagous when adults (Acuña et al., 2005). Swimming mode is carangiform (Link and Habit, 2015) and during the reproductive season this species swims in schools (Vila et al., 1981). Genetic and mark-recapture data suggests that this species exhibits extensive movements along rivers (Victoriano et al., 2012; Piedra et al., 2012).

Cheirodon galusdae also inhabits the piedmont of the Andes and Central Valley from 35 to 39° latitude south (Dyer, 2000). Maximum body size is 90 mm when adult, and swimming mode is subcarangiform (Link and Habit, 2015). Its reproductive season occurs from late spring to summer, but spawning and rearing habitats are unknown. *Cheirodon galusdae* feeds on periphyton and epizoon communities and inhabit in lakes and shallow vegetated ponds in rivers (Ruiz, 1993; Habit et al. 2006). There is no data about its movement patterns.

Conservation status of both species is Vulnerable (Vila and Habit, 2015). Endurance was described for both species by Laborde et al. (2016), finding that both species performance was very similar (Figure 1).

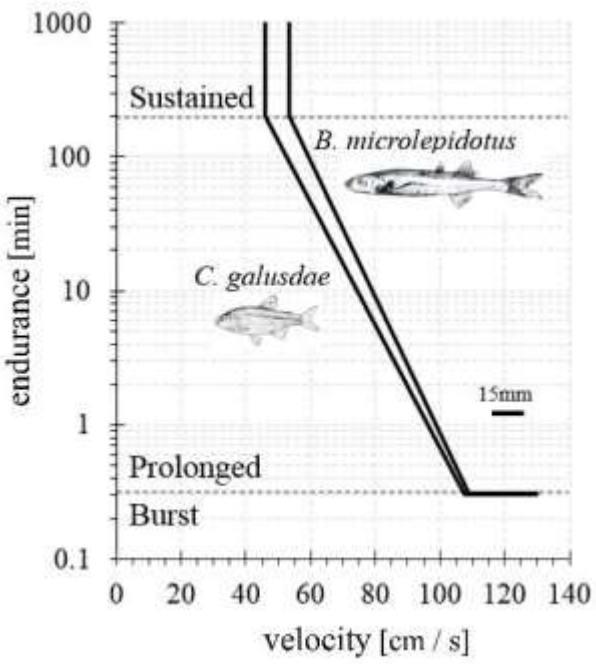

Fig. 1. Endurance curves for *C. galusdae* and *B. microlepidotus* (after Laborde et al., 2016).

Fish were collected from the Itata River (at 36°45'30"S, 72°24'53"W) using a backpack electroshocker (Smith-Root LR24, Vancouver, WA, USA) and seine net (2-mm mesh). All collected fish were transported to glass aquariums at the Hydraulics and Environmental Engineering Laboratory of the University of Concepción. To avoid mortality, guidelines for fish transportation and successful maintenance in captivity of Chilean native fish were followed (Sobenes et al., 2012). Fish were kept for at least 15 days before experiments. Fish were fed *ad libitum* with live prey (macroinvertebrates from streams and *Enchitrea* sp., *Tenebrio molitor*, and *Eisenia foetida*) three or four times a week according to Sobenes et al. (2012) and García et al. (2012). Following Jobling (1982) feeding was interrupted 48 h before each experiment. Water temperature was kept stable at 17±1°C for 1 week before the experiment. A total of 12 individuals (6 *C. galusdae* and 6 *B. microlepidotus*) of similar

150 body length (44.8 ± 1.5 mm for *C. galusdae* and 77.7 ± 5.9 mm for *B. microlepidotus*) were
151 tested.
152
153 *2.2 Experimental installation*
154 Experiments were conducted in a laboratory flume 6 m length, 40 cm width, and 40 cm
155 height located at the Hydraulic Engineering Laboratory of the University of Concepción. A
156 honeycomb matrix was placed at the flume entrance to provide an aligned flow. An
157 interrogation area of 0.65 m length, located 2.5 m downstream from the entrance was
158 isolated with a net in order to keep fishes in the interrogation area. Vertical mounted
159 cylinders with diameters of 2, 3, 4, 5 and 6 cm were placed at the upstream end of the
160 interrogation area. The discharge *Q* was controlled by a variable frequency drive (VFD)
161 and measured with an electromagnetic flow meter having an accuracy of ±0.5%. The flow
162 depth, *h*, was controlled by adjusting the tailgate at the end of the flume, and was measured
163 with an ultrasonic distance sensor (UDS). (Figure 2).

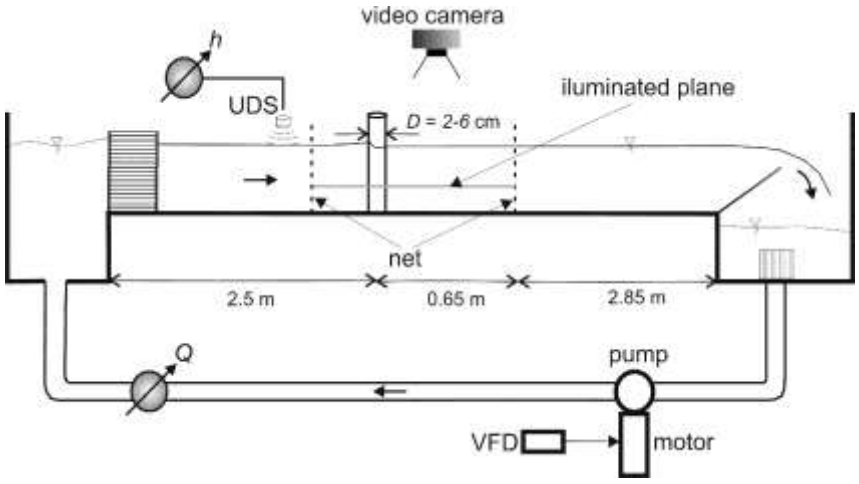

164
165 **Fig. 2.** Scheme of the experimental installation.
166

167 *2.3. Particle Image Velocimetry*

168 The flow field was characterized using a two dimensional Particle Image Velocimetry
169 (PIV) measurement system in order to determine the vortex shedding frequencies f and
170 corresponding length scale, L_u at the cylinder wakes. Measurements were performed at a
171 horizontal plane located at a height of 40% of the flow depth. The particle seeding density
172 was carefully designed to allow the recommended minimum of ~5 particles in each
173 interrogation window (Adrian and Westerweel, 2011). A Sony Action Cam HDR-
174 AS100V® with a 32GB memory, 1280x720 pix resolution and acquisition frequency of
175 120 Hz was used to record the particle motion. For the flow conditions analyzed, the 120
176 Hz allowed displacements between frames larger than the particle diameter in the images,
177 thus errors produce by short displacements were minimized. These displacements were also
178 long enough to allow a good correlation peak magnitude in the correlation analysis. To
179 ensure statistical convergence, the flow field was measured during 7 minutes, i.e. 50400
180 frames.

181 Before the measurements, but using the same experimental conditions, a target
182 containing reference marks was placed in the flow channel at same position as the light
183 plane. Images of the target were used to correct the PIV images for typical barrel and
184 pincushion lens distortions, but also to correct optical deformations induced by the
185 experimental setup. After the PIV processing was completed, the displacements in camera
186 coordinates (pix) were converted to real world coordinates (cm) using also the information
187 provided by the calibration target. An enclosure around the flume was built to avoid the
188 recording of environmental light in the images. Analogously to the work by Gross et al.
189 (2010) two sources of light were used as the light density of a single one was not enough to

produce a good contrast level in the images. The light was collimated to illuminate a flow region of 20 cm-long and 0.8 cm-wide. Polyamide-12 particles of 100 μm diameter and 1.06 g/cm^3 density were used as tracers. The size and density of these particles ensure that they will respond to a wide range of flow structures of interest (Melling, 1997).

Tracer displacement was calculated using the toolbox for Matlab, PIVlab® developed by Thielicke and Stamhuis (2014a,b). A multi-pass approach with final interrogation windows of 32 x 32 Pix was used for the calculations. With the aim of improving the velocity estimation in high shear regions, the image deformation technique was used (Scarano, 2001). The displacement calculation was improved using a Gaussian subpixel accuracy estimation (Adrian and Westerweel, 2011). The percentage of outlier vectors in individual frames was always less than the 4~5% recommended (Adrian and Westerweel 2011). During the post processing of the estimated velocity fields, the universal outlier filter of Westerweel and Scarano (2005) was used for outlier removal, while a cubic interpolation technique was used for their estimation.

2.3.1 Vortex shedding frequency

Time series of the spanwise velocity component were extracted from the PIV measurements and a Fourier analysis was performed for determination of the dominant frequencies corresponding to shedding frequencies of the wake vortices. The power spectra density, E_v was calculated for each experiment applying the Fourier transform to the spanwise velocity autocorrelation function $R_v(\tau)$ of the velocity fluctuations v':

$$R_v(\tau) = \overline{v'(x,t)v'(x,t+\tau)} \quad (1)$$

$$E_v = \frac{1}{2}\pi \int_{-\infty}^{\infty} e^{-if\tau} R_v(\tau)\partial\tau \quad (2)$$

The Fourier transform decompose the autocorrelation signal into a family of frequencies, where each frequency is associated with a different energy level. Peaks of the power spectra density correspond to dominant frequencies. In this case, the vortex shedding frequency correspond to the maximum spectral peak. The method of Welch (Welch, 1967) as implemented in the signal processing toolbox of Matlab was used for the calculations.

2.3.2 Vortex length scale

The integral vortex length scale is L_u=D, with D the cylinder diameter. With additional assumptions (Taylor, 1935), vortex length scale is given by $L_u = U / f$, where f is the shedding frequency.

2.4. Fish behavior and tail beat kinematics

Video records of fish motion with 20 minutes duration were analyzed to characterize the fish behavior and the tail beat kinematics following the methodology by Oufiero et al. (2014). Fish were recorded dorsally at 120 fps using a Sony Action Cam HDR-AS100V®. The images obtained with this camera were also corrected for optical distortions.

For determination of tail beat amplitude (λ) and tail beat frequency (f_{TB}) videos were digitized using the software ImageJ (U.S. National Institutes of Health, Bethesda, Maryland, USA, http://imagej.nih.gov/ij/). The base of the caudal fin was digitized for

consecutive full tail beats taken from portions of the swimming trials with minimal movement of the fish centroid. This point was digitized when the tail was extended maximally laterally, on either side for each of the full tail beats (Fig. 3).

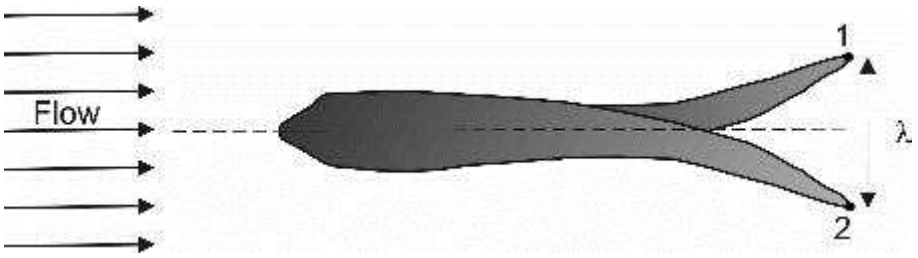

Fig. 3. Digitized points (1 and 2) for determination of the tail beat amplitude λ.

Horizontal and vertical coordinates for each video and trial were further processed to obtain the average tail beat amplitude and timing. Tail beat time was the time it took for one complete tail beat cycle, from maximal lateral position on the right side of the fish, through the center position, to the maximum lateral position on the left side of the fish, and back to the original starting position on the maximum lateral right side. From these two observations, tail beat frequency f_{TB} was calculated, i.e. the inverse of the tail beat time was calculated, giving an estimate of the number of tail beats per second. In order to quantify the propulsion effort in terms of tail beats the average tail beat frequency f_{TB}^{30} corresponding to 30 tail beats was analyzed. The fish Strouhal number, $St_{fish} = f_{TB}^{30} \lambda / U$, was then determined. U is the section averaged flow velocity.

2.5. Experimental series

252 Six individuals of each study species, having similar body length (BL) and critical
253 swimming speed, were tested with free flow, and with five cylinders having diameters of 2,
254 3, 4, 5, and 6 cm. S1 was the reference series with free flow experiments. Series S2 and S3
255 served to investigate behavior and tail beat kinematics of *C. galusdae* and *B.*
256 *microlepidotus* in the presence of cylinders, respectively. In series S2 and S3, individuals
257 were exposed to repeated tests, being exposed to wakes caused by the cylinder of 2, 3, 4, 5,
258 and 6 cm in diameter. Conditions for each of the 72 experiments are included as
259 supplementary material. Each trial began with 1.5 hours of acclimatization with a section
260 averaged velocity of 1 BL/s in order to decrease the stress produced on the fish.
261 Subsequently, flow velocity was slowly raised up to the tested condition. In order to avoid
262 fish fatigue, in all experiments the section averaged flow velocity was equal 0.7 times the
263 critical swimming speed of the individual, U_{cr} (Webb, 1971), which was reported by
264 Laborde et al. (2016). In order to confirm this assumption variation of tail beat frequency at
265 the beginning and end of the experiments was compared with the Wilcoxon Matched Pair
266 Test. The experiments spanned cylinder Reynolds number $Re_D = \rho UD / \mu$, where ρ is the
267 fluid density, U the section averaged flow velocity, D the cylinder diameter and μ the
268 dynamic viscosity of water, in the range of 3000 to 17000 and cylinder Strouhal number St
269 $= f D / U$, where f is the shedding frequency from 0.17 to 0.21.

270 Tail beat frequency, tail beat amplitude and fish Strouhal number were compared
271 between the two species with a one-way Analysis of Variance (ANOVA) prior verification
272 of variance and normality homogeneity tested by the Levene and the Kolmogorov-Smirnov
273 test, respectively. Significant differences of the tail beat kinematics and fish Strouhal in
274 wakes and free flow for each species were tested using a Friedman ANOVA χ^2 test.

Tendencies of the aforementioned variables with flow properties such as the relative vortex size and vortex shedding frequency were analyzed fitting linear or potential regressions.

3. Results

3.1. Flow properties

The angle of flow separation, α at the cylinder wakes was computed from the Reynolds stress distributions as illustrated in Fig. 4 (a). In all cases $\alpha = 15° \pm 1°$. The point of merging of the two separated shear layers in Fig. 4 (a) can be identified as the location of the peak of the TKE profile at the longitudinal centerline position in Fig. 4 (b). For small diameters the distance of the TKE peak to the cylinder slightly increases. After the TKE peak almost a linear decay of the TKE with the downstream direction is observed, which occurs as a consequence of the diffusion of the wake vortices, or in other words occurs as a consequence of the processes responsible of recovering the channel flow condition. Figures 4 (c) and 4 (d) shows the autocorrelation function and corresponding spectral peak in experiment S3-19 according to Eqs. (1) and (2). From the figure 4 (d) the dominant frequency is 0.7 Hz.

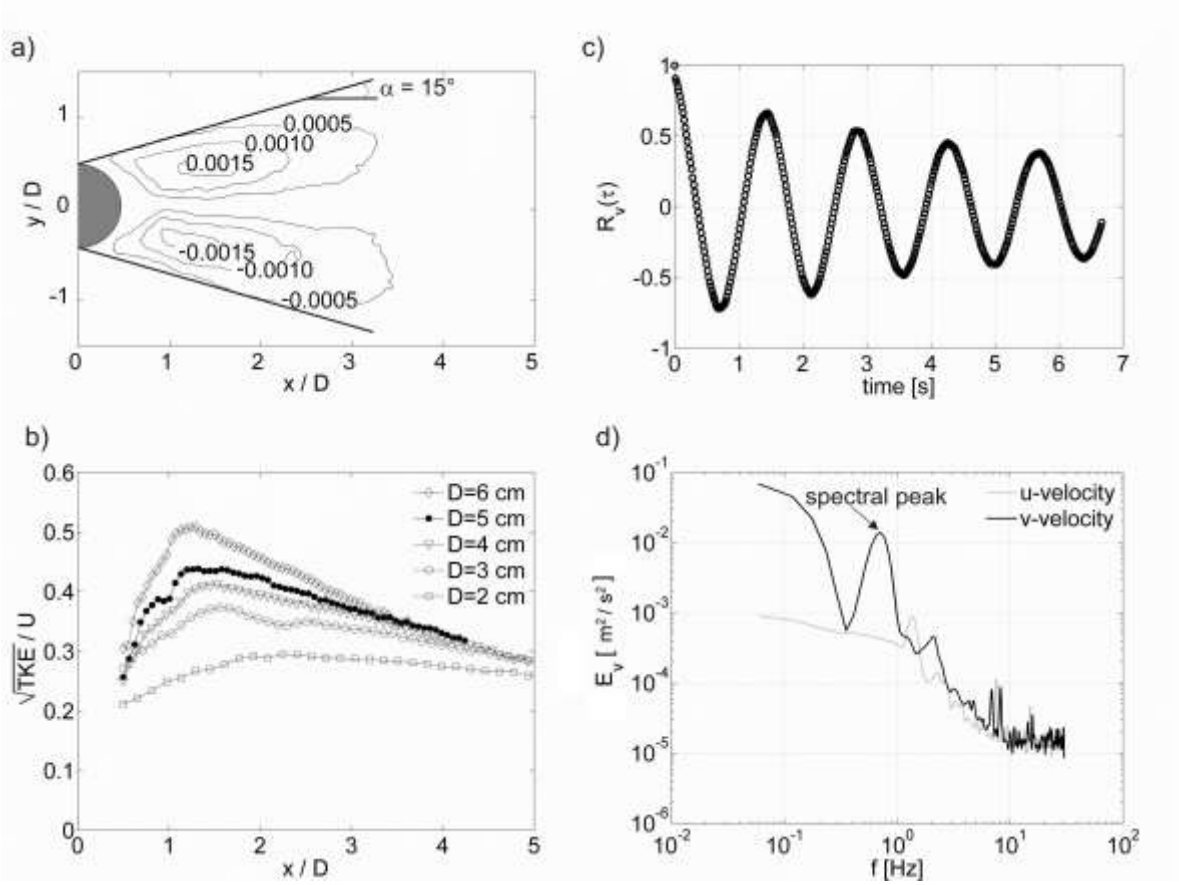

Fig. 4. a) Normalized Reynolds stresses $\overline{v'u'}/U^2$, b) profiles of Turbulent Kinetic Energy along the centerline, c) spanwise velocity autocorrelation function, and d) power spectral density for experiment S3-19.

Table 1 in Suppl. Material includes frequency for each experiment. Cylinder wakes were found in the so-called shear-layer transition regime with Kelvin-Helmholtz instabilities which occurs in the range $1000 < Re_D < 100{,}000$ (Williamson 1996). The wake vortices were shed on a vertical axis at a dominant frequency described by the cylinder Strouhal number. In the experiments the observed relationship between Re_D and St followed the curve proposed by Fey et al. (1998):

$$St = \begin{cases} 0.2040 + \dfrac{0.3364}{\sqrt{Re_D}} & 1300 < Re_D < 5000 \\ 0.1776 + \dfrac{2.2023}{\sqrt{Re_D}} & 5000 < Re_D < 2 \cdot 10^5 \end{cases} \quad (3)$$

3.2. Fish behavior

Video records of fish motion during the experiments revealed that both studied species interacted with vortices with different consequences for swimming kinematics, i.e. propulsion effort associated with the movement of the caudal fin (see supplementary material). In the free flow condition, *C. galusdae* exhibited a burst-and-coast swimming style. In general, all analyzed individuals of this specie avoided the cylinder wakes, searching for more favorable flow conditions (i.e., less swimming effort) in the interrogation area. During the experiments with cylinders >2 cm in diameter, *C. galusdae* diminished the coast phase respect to the free flow, reducing it with the vortex length scale towards zero, and when entering in these wakes clear destabilization was observed (See Video 1 in supplementary material). In this context, destabilization was considered to have occurred when the fish was displaced downstream, accompanied by lateral displacement and loss of heading, despite increasing tail beat frequency (Tritico & Cotel, 2010; Maia et al., 2015).

In contrast, *Basilichthys microlepidotus* swam holding position in free flow, and in the cylinder wakes (See Video 2 in supplementary material). Its lateral body displacement in the cylinder wake was consistent with the width of the wake (Figure 4) as observed for

Kármán gaiting (Liao et al., 2003a; Liao et al., 2003b; Liao et al., 2007; Taguchi and Liao, 2011).

3.3. Tail beat kinematics

During experiments tail beat frequency did not show a trend of change with time (See Figure 1 in Supplementary material). Additionally, no significant differences in average tail beat frequency in free flow and wake were observed (Wilcoxon Matched Pair Test was Z = 0,943, p = 0,345 for *C. galusdae*, and Z = 1,153, p = 0,248 for *B. microlepidotus*). This results support that no time effect related to fatigue occurred in the experiments. Detailed information is included as supplementary material.

3.3.1 Tail beat frequency, f_{TB}

Cheirodon galusdae adopted a burst-and-coast swimming style. Typically, a burst phase consisted of 5 to 20 tail beats, and thus for individuals of *C. galusdae* the average tail beat frequency, f_{TB}^{30} included several burst and coast phases. *Basilichthys microlepidotus* used the caudal fin for propulsion continuously and thus f_{TB}^{30} was constant. f_{TB}^{30} was significantly higher in *C. galusdae* (8.18 ± 1.30 SD) than in *B. microlepidotus* (4.87 ± 0.41 SD) (one way ANOVA, $F_{(1,70)}= 77.35$, $p < 0.001$).

Different tendencies of f_{TB}^{30} with the relative vortex size L_u / L and with vortex frequency f were observed for both species (Fig. 5). *Cheirodon galusdae* in cylinder wakes presented higher values of f_{TB}^{30} than in the free flow case, up to 52% (ANOVA χ^2=19.37,

341 p<0.001). By the contrary, *B. microlepidotus* presented similar values of f_{TB}^{30} in free flow
342 and in cylinder wakes (ANOVA χ^2=4.47, p=0.48).

343 The tail beat frequency of both species did not change significantly with the flow
344 properties, i.e. relative vortex size (R^2=0.084, p=0.119 for *C. galusdae* and R^2=0.029,
345 p=0.365 for *B. microlepidotus*) and vortex shedding frequency (R^2=0.107, p=0.077 for *C.*
346 *galusdae* and R^2=0.021, p=0.447 for *B. microlepidotus*).

347

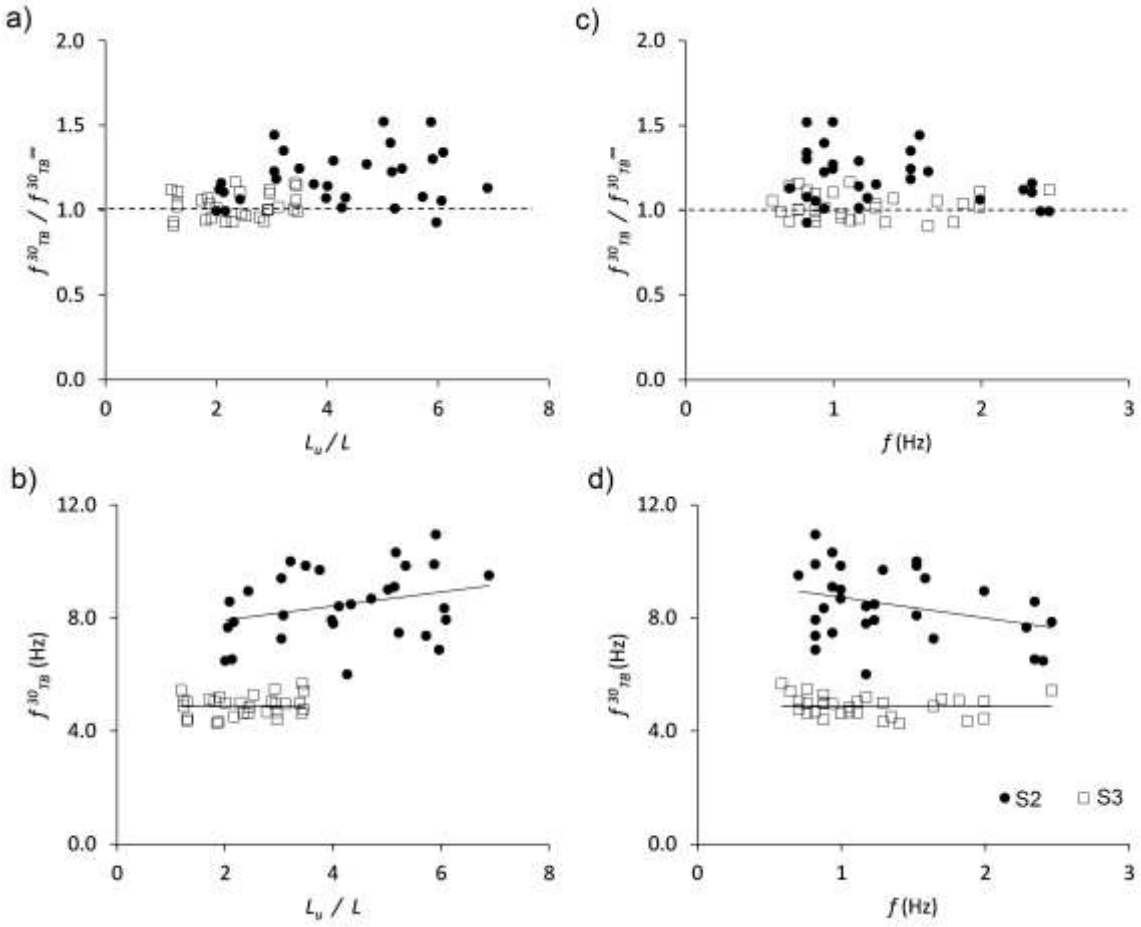

348

349 **Fig. 5.** a) Average tail beat frequency, f_{TB}^{30} divided by average tail beat frequency in the
350 reference series S1 with free flow, f_{TB}^{∞} over relative vortex size L_u / L. b) f_{TB}^{30} over relative

vortex size L_u / L. c) f_{TB}^{30} divided by f_{TB}^{∞} over vortex frequency f, and d) f_{TB}^{30} over f for experiments of series S2 (circles) and S3 (squares). Grey dashed lines indicate the free flow condition for reference. Black, solid lines show the observed tendencies.

3.3.2. Tail beat amplitude

Relative tail beat amplitude λ^* (normalized with the fish length, $\lambda^* = \lambda / L$) was significantly higher in *C. galusdae* (0.28 ± 0.03 SD, and 0.21 ± 0.03 SD for *B. microlepidotus*; one way ANOVA, $F_{(1,70)} = 72.41$, $p < 0.001$). The tail beat amplitude showed a significant increase for individuals of both species in the cylinder wake respect to the free flow case, up to 55% (χ^2=21.38, p<0.001 for *C. galusdae*, and χ^2=22.26, p<0.001 for *B. microlepidotus*) (Figure 6). Tail beat amplitude ranged between 0.16 and 0.37 times the fish length with a mean value of λ =1.26 ± 0.17 SD for *C. galusdae* and λ =1.64 ± 0.19 SD for *B. microlepidotus*. For both species λ^* increased with the relative vortex size L_u / L following a potential relationship $\lambda^* = a(L_u/L)^b$ (a=0.180, b=0.296, R^2=0.561, p<0.001), and decreased linearly with vortex frequency f, following $\lambda^* = m + nf$ (m=0.337, n=-0.039, R^2=0.371, p<0.001 for *C. galusdae*, and m=0.271, n=-0.043, R^2=0.464, p<0.001 for *B. microlepidotus*).

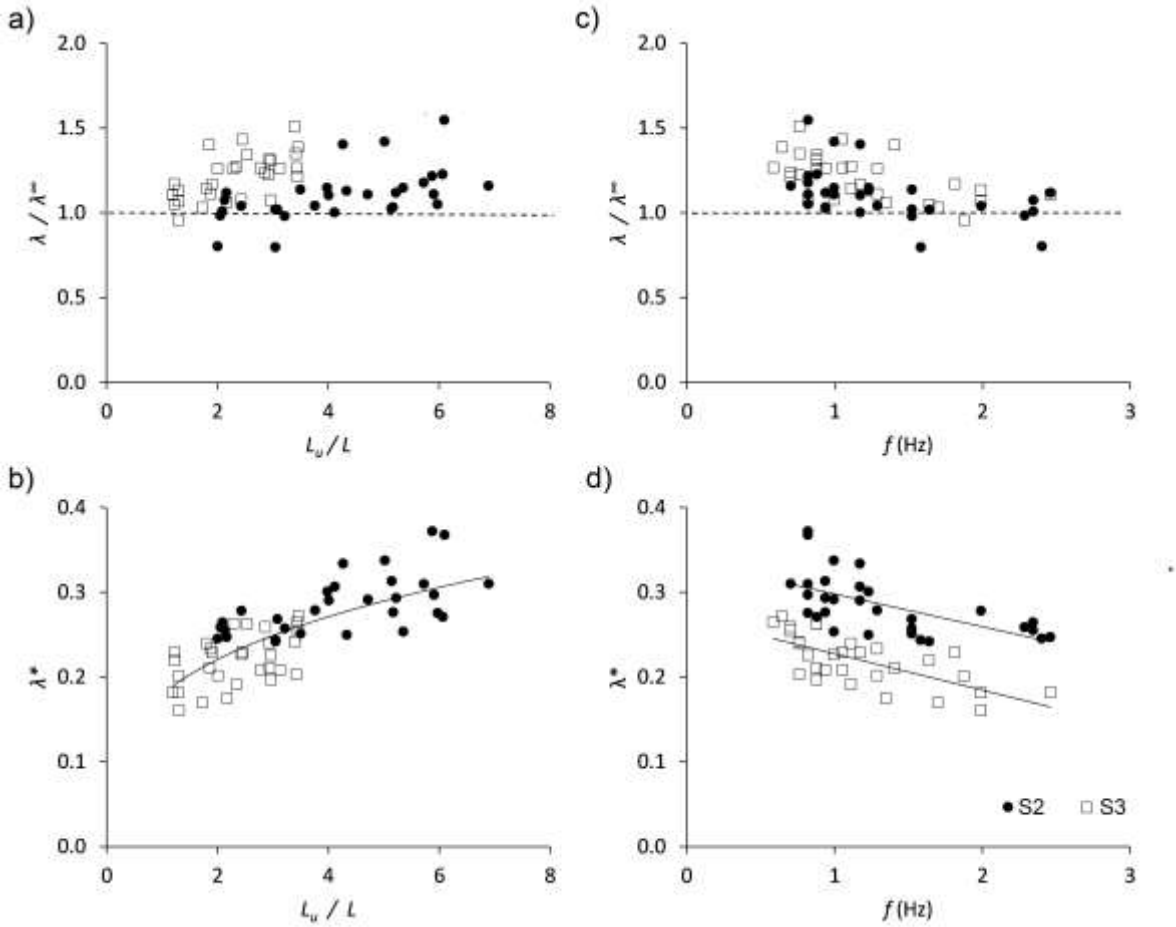

Fig. 6. Tail beat amplitude, λ divided by tail beat amplitude in reference series S1 with free flow, λ^{∞} over relative vortex size L_u / L, (with $L_u = U / f$). b) Normalized tail beat amplitude λ^* (relative to the fish length, L) over L_u / L. c) Tail beat amplitude, λ divided by tail beat amplitude in reference series S1 with free flow, λ^{∞} over vortex frequency f, and d) normalized tail beat amplitude λ^* over f for experiments of series S2 (circles) and S3 (squares). Grey dashed lines indicate the free flow condition for reference. Black, solid lines show the observed tendencies.

3.4. Fish Strouhal number, St_{fish}

379 St_{fish} showed no statistical differences between the two species (0.48 ± 0.10 for *C.*
380 *galusdae* and 0.43 ± 0.11 for *B. microlepidotus*; one way ANOVA, $F_{(1,70)} = 3.30$, p =
381 0.071).

382 In the free flow case fish Strouhal number St^{∞}_{fish} ranged from 0.29 to 0.50 with a value
383 of 0.38 ± 0.08 SD, while in the cylinder wakes St_{fish} ranged from 0.28 to 0.80 with a 0.47 ±
384 0.11 SD. The fish Strouhal number in cylinder wakes was significantly higher than in free
385 flow (χ^2=17.90, p=0.003 for *C. galusdae*, and χ^2=17.78, p=0.0014 for *B. microlepidotus*)
386 (Fig. 7).

387 For both species St_{fish} increased with the relative vortex size following a potential
388 relationship $St_{fish} = a\left(L_u / L\right)^b$ (a=0.356, b=0.235, R^2=0.232, p<0.001), and decreased with
389 vortex frequency f, following a potential relationship $St_{fish} = af^b$ (a=0.481, b=-0.296,
390 R^2=0.248, p<0.001). Neither a significant correlation of St_{fish} with the cylinder Reynolds
391 number Re_D nor with the flow Strouhal number St was observed (p=0.147 and p=0.304,
392 respectively).

393

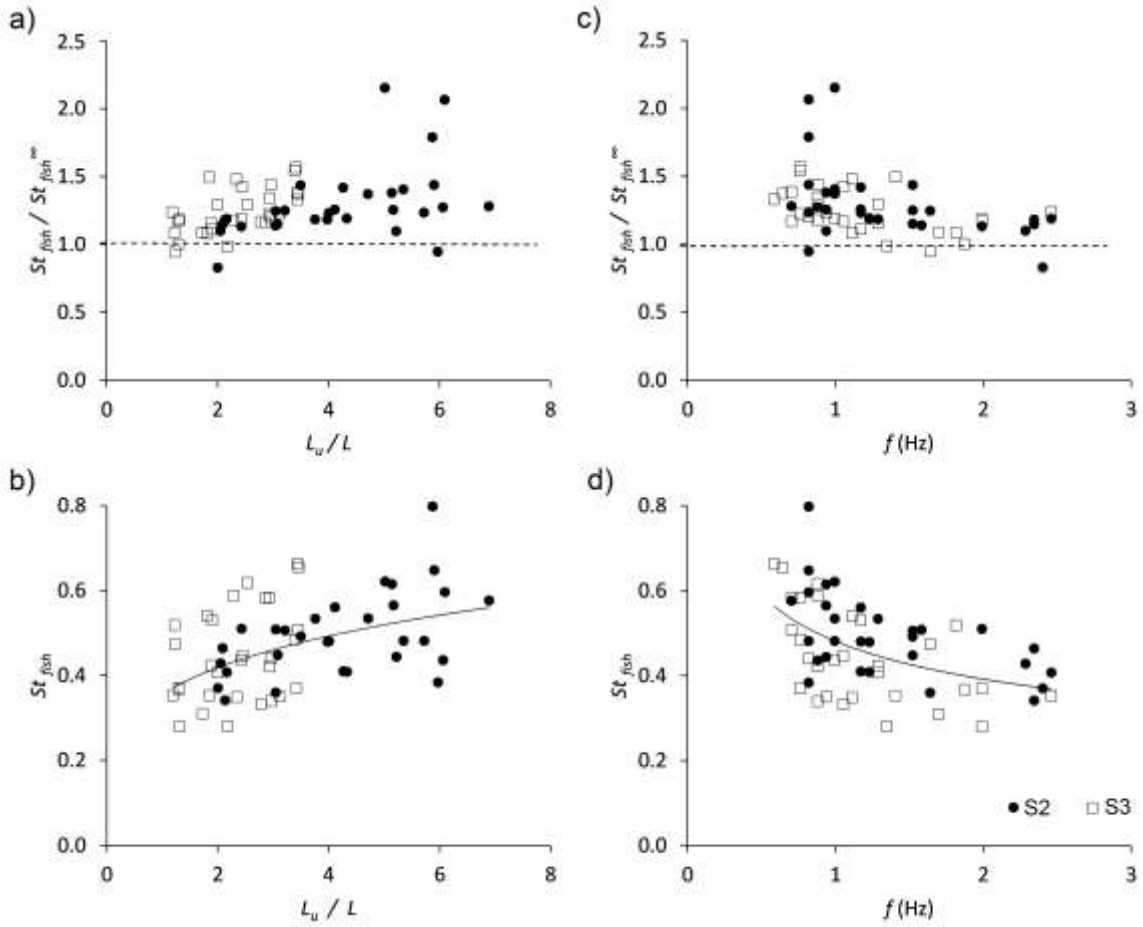

394

395 **Figure 7.** a) Fish Strouhal number, $St_{fish} = f_{TB}^{30} \lambda / U$ divided by the fish Strouhal number in

396 the reference series S1, St_{fish}^{∞}, over relative vortex size L_u / L, b) St_{fish} over L_u / L, c)

397 $St_{fish} / St_{fish}^{\infty}$ over f, and d) St_{fish}^{∞} over f, for experiments of series S2 (circles) and S3 (squares).

398 Grey dashed lines indicate the free flow condition for reference. Black, solid lines show the

399 observed tendencies.

400

401 **4. Discussion**

Experiments on behavior and tail beat kinematics of fish swimming in a cylinder wake were analyzed in the context of fishway design criteria. A total of six individuals of *C. galusdae* and six individuals of *B. microlepidotus* (juveniles) were tested in a reference condition with free flow, and in the wake of cylinders having 2, 3, 4, 5, and 6 cm diameter. In all experiments, the average flow velocity was 0.7 times the critical swimming speed for each species, avoiding fish fatigue. Individuals had lengths that correspond to the standarized critical swimming speed and in this sense, they were representative of the species (Laborde et al. 2016). Individuals of each study species were selected to have similar body lengths, and thus they were considered replicates of the behavioral responses to turbulent wakes.

Our results demonstrate the difficulties in establishing realistic hydraulic design criteria for multispecies fishways based on critical swimming speed and endurance curves only, due to the divergent swimming style and performance exhibited by the two species in the altered flows, i.e. cylinder wakes. As currently guidelines for hydraulic design of fishways are based on criteria suitable for relatively strong-swimming species with migratory behavior, such as salmonids (Katopodis and Williams, 2012), further development of fish passage technology is especially needed for non-sport fish (Link and Habit, 2015). The main reasons are: (i) although many non-sport fish do not exhibit strong migration patterns, they do need to perform local movements to complete their life cycles (Piedra et al., 2012) and maintain idiosyncratic patterns of gene flow within river networks (Victoriano et al., 2012); (ii) the small body length of non-sport fish limits absolute swimming speeds (i.e. not relative to body length) (*e.g.* Mitchell, 1989; Nikora et al., 2003; Plew et al., 2007; Laborde et al., 2016); and (iii) depending on turbulence swimming performance may be enhanced,

425 diminished or unaffected in altered flows (Lacey et al., 2012; Wilkes et al., 2013; Enders
426 and Boisclair, 2016).

427 In nature, *B. microlepidotus* juveniles inhabit shallow riparian zones and littoral zones
428 (Link and Habit, 2015), moving to the main current with maturity (Montoya et al., 2012).
429 This ontogenetic shift in habitat use might explain its high swimming capacity relative to
430 body length (Laborde et al., 2016). In our experiments, *B. microlepidotus* adopted a
431 distinctive swimming gait by attuning its body amplitude to match the structure of the
432 classic von Kármán vortex street found downstream of a bluff body. Tail beat amplitude
433 increased with vortex length scale, and the lateral movement of the fish centroid in the
434 wake was consistent the wake width. This indicates that *B. microlepidotus* was adopting a
435 Kármán gait-like swimming strategy, thus reducing swimming costs in the cylinder wake.
436 However, differently to rainbow trout (*Onchorhynchus mykiss*) (Liao et al., 2003a; Liao et
437 al., 2003b; Liao et al., 2007; Taguchi and Liao, 2011) in the presence of cylinders, *B.*
438 *microlepidotus* did not attune its tail beat frequency to the shedding frequency. One
439 possible reason is that vortex length scale to fish length ratio was too high (for *O. mykiss*
440 the special conditions required for Kármán gaiting may be limited to $0.25 < L_u / L < 0.5$,
441 while in our experiments $L_u / L > 1.2$). Even though *B. microlepidotus* in wakes did not
442 change the tail beat frequency respect to the free flow, it increased the tail beat amplitude
443 with the relative vortex length scale, evidencing a higher propulsion effort using the caudal
444 fin. Further research in order to investigate if *B. microlepidotus* can gain an energetic
445 advantage in the wake of a cylinder, by reducing muscle activity and oxygen consumption
446 in comparison to swimming in the free flow, is needed.

447 In our experiments mean flow velocity was equal to 70% of the critical swimming
448 speed of the individual. In nature, however, *C. galusdae* inhabits vegetated riparian zones
449 with lower flow velocities (Link and Habit, 2015), swimming intermittently to hold
450 position. Contrary to this behavior in nature, during experiments *C. galusdae* adopted a
451 burst-and-coast swimming strategy often observed in fish with a fineness ratio of 4–6.5
452 (Videler 1993). Studied individuals of *C. galusdae* presented fineness ratios of 4. In the
453 presence of cylinders >2 cm in diameter, *C. galusdae* reduced the coast phase dramatically,
454 swimming quasi-continuously and suffering destabilization and displacement. Average tail
455 beat frequency f_{TB}^{30} as well as tail beat amplitude increased with relative vortex length
456 scale. Even though the burst-and-coast swimming style has been shown to save up to 45%
457 of the energy due to drag reduction in the coast phases (Wu et al. 2007, Chung 2009) our
458 results suggest that, under the studied conditions, *C. galusdae* increased propulsion effort in
459 the cylinder wake due to coast phase reduction. It is not clear if the swimming behavior
460 observed in *C. galusdae* constitutes aerobic or anaerobic activity. Therefore, further work
461 on muscle activity and oxygen consumption is also required for this species.

462 The fish Strouhal number defined in terms of the average tail beat frequency f_{TB}^{30}, the
463 tail beat amplitude λ, and the section averaged flow velocity U can be interpreted as a
464 measure of the propulsion effort. Extensive observations have shown that maximum
465 propulsive efficiency lies in the range $0.25 < St_{fish} < 0.35$ for a diversity of fish species
466 (Triantafyllou et al., 1993; Eloy, 2012). In our study, both species converged towards this
467 range with decreasing relative vortex size and corresponding higher shedding frequencies,
468 following one tendency even when the two species adopted very different swimming

469 strategies, i.e. Kármán gait-like and burst-and-coast. This would support the idea that in the
470 sense of propulsion effort, *B. microlepidotus* in a wake is expending more effort than in a
471 free flow, similar to *C. galusdae*. Probably, the similar propulsive effort observed through
472 Strouhal number for both species is related to their similar swimming capacity, and thus
473 species with significantly different swimming capacity (critical swimming speed,
474 endurance) might be expected to exhibit different relations of St_{fish} with vortex length scale
475 and shedding frequency. Overall, the fish Strouhal number appears to be a suitable design
476 criterion, as it compiles the propulsion effort of fish in a flow (free and/or altered) and
477 could be limited to manage propulsion efficiency of different species in a fishway. Energy
478 saving mechanisms associated with Kármán gaiting could counteract the additional effort in
479 propulsion exhibited by *B. microlepidotus*, and should constitute additional/complementary
480 criteria for fishway design.

481 Fish behavior in wakes is species-specific. The intensity, periodicity, orientation and
482 scale of wake vortices are expected to influence fish behavior and swimming performance
483 since they are critical for fish maneuvering and swimming stability (Lacey et al., 2012;
484 Wilkes et al., 2013; Maia et al., 2015). Cylinder wakes represent a special case of
485 turbulence which is significantly different to the free flow turbulence due to the periodicity
486 and location of the vortices, it is a two-dimensional case with homogeneous properties
487 along the water column. In the present study, experiments were conducted under similar
488 flow conditions to those expected in real fishways, i.e. average flow velocity was 70% of
489 the critical velocity being in the sustained swimming mode (Webb, 1971). *Basilichthys*
490 *microlepidotus* appeared to be adapted to swimming in wakes, while *C. galusdae* did not.
491 Obstacles with different shapes however produce wakes with more complex vortices. In

fish ramps, submerged boulders produce wakes with a marked three-dimensional shape (Bretón et al., 2013; Baki et al., 2014) and lower periodicity, i.e. predictability, than the studied cylinder wakes. Therefore, in comparison to the cylinder case, a wake at a submerged boulder is thought less predictable for a fish.

5. Conclusions

The behavior and tail beat kinematics of two non-sport fish species from Chile, *C. galusdae* and *B. microlepidotus* (juveniles), was studied in the wake of vertical and bottom-mounted cylinders in an open channel flow through Particle Image Velocimetry and videography of fish motion.

Cheirodon galusdae was often destabilized in cylinder wakes and adopted an erratic burst-and-coast like swimming style, decreasing the coast phase in the presence of cylinders >2 cm in diameter. *Basilichthys microlepidotus* adopted a Kármán gait-like swimming strategy, interacting with the wake vortices, but without attuning its tail beat frequency to the shedding frequency, and increasing its tail beat amplitude with vortex length scale. These findings suggest that *C. galusdae* and *B. microlepidotus* may increase energetic costs when swimming in altered flows with vortex length scale to fish length ratios as those in the present study.

The fish Strouhal number provided a good measure of propulsion effort and seems to be a practical design criterion. Energy saving mechanisms (e.g. those associated with Kármán gaiting) could counteract the additional propulsive effort, and should constitute additional/complementary criteria.

514 Life histories provided a possible explanation to the main observed differences
515 between species behavior but further research is required in order to link the physiological
516 characteristics of non-sport fish with swimming performance in wakes.
517
518

519 **ACKNOWLEDGEMENTS**

520 The financial support provided by the Chilean Research Council CONICYT through
521 Grant FONDECYT 1150154: 'Within-basin barriers and among-basin leaks: changing
522 connectivity of rivers in central Chile and its impact on native fish' is greatly
523 acknowledged. So too is the support of HORIZON 2020 EU initiative through project
524 'Knowledge Exchange for Efficient Passage of Fishes in the Southern Hemisphere'
525 (H2020-MSCA-RISE-2015-690857-KEEPFISH). EH and OL are supported by Red 14
526 Doctoral REDOC.CTA, MINEDUC project UCO1202 at U. de Concepción. Finally, many
527 thanks go to Jorge González for his help in collecting fish, to René Iribarren and Daniela
528 Baeza for their collaboration during the experimental work, and to Karina Reyes, Daniela
529 Baeza and Patricio Rubilar for their collaboration with the processing of digital video-
530 images and analysis.

531

532

533

References

Acuña, P., Vila, I., Pardo, R., Comte, S., 2005. Caracterización espacio-temporal del nicho trófico de la fauna íctica andina del río Maule, Chile. Gayana, 69: 175-179.

Adrian, R. J., Westerweel, J., 2011. Particle image velocimetry (No. 30). Cambridge University Press.

Bainbridge, R., 1958. The speed of swimming of fish as related to size and to the frequency and amplitude of the tail beat. Journal of Experimental Biology, 35(1), 109-133.

Baki, A. B. M., Zhu, D. Z., Rajaratnam, N., 2013. Mean flow characteristics in a rock-ramp-type fish pass. Journal of Hydraulic Engineering, 140(2), 156-168.

Baki, A. B. M., Zhu, D. Z., Rajaratnam, N., 2014. Turbulence characteristics in a rock-ramp-type fish pass. Journal of Hydraulic Engineering, 141(2), 04014075.

Bretón, F., Baki, A. B. M., Link, O., Zhu, D. Z., Rajaratnam, N., 2013. Flow in nature-like fishway and its relation to fish behaviour. Canadian Journal of Civil Engineering, 40(6), 567-573.

Brown, J. J, Limburg, K. E., Waldman, J. R., Stephenson, K., Glenn, E. P., Juanes, F., Jordaan, A., 2013. Fish and hydropower on the U.S. Atlantic coast: failed fisheries policies from half-way technologies. Conservation Letters 6: 280-286.

Bunt, C. M., Castro-Santos, T., Haro, A., 2012. Performance of fish passage structures at upstream barriers to migration. River Research and Applications, 28(4), 457-478.

Butchart, S.H., Walpole, M., Collen, B., Van Strien, A., Scharlemann, J.P., Almond, R.E., Baillie, J.E., Bomhard, B., Brown, C., Bruno, J., Carpenter, K.E., 2010. Global biodiversity: indicators of recent declines. Science, 328(5982), 1164-1168.

556 Castro-Santos, T., Cotel, A. L., Webb, P. W., 2009. Fishway evaluations for better
557 bioengineering: an integrative approach. In: Challenges for diadromous fishes in a
558 dynamic global environment. American Fisheries Society, Symposium, Vol. 69, 557-
559 575.
560 Chung, M. H., 2009. On burst-and-coast swimming performance in fish-like
561 locomotion. Bioinspiration & Biomimetics, 4(3), 036001.
562 Dyer, B., 2000. Systematic review and biogeography of the freshwater fishes of
563 Chile. Estudios Oceanológicos, 19, 77-98.
564 Eloy, C., 2012. Optimal Strouhal number for swimming animals. Journal of Fluids and
565 Structures, 30, 205-218.
566 Enders, E. C., Boisclair, D., 2016. Effects of environmental fluctuations on fish
567 metabolism: Atlantic salmon Salmo salar as a case study. Journal of Fish Biology, 88(1),
568 344-358.
569 Feurich, R., Boubée, J., Olsen, N. R. B., 2012. Improvement of fish passage in culverts
570 using CFD. Ecological Engineering, 47, 1-8.
571 Fey, U., König, M., Eckelmann, H., 1998. A new Strouhal-Reynolds-number relationship
572 for the circular cylinder in the range $47 < Re < 2\times10^5$. Physics of Fluids, 10, 1547-1549.
573 García A, Sobenes C, Link O, Habit E., 2012. Bioenergetic models of the threatened darter
574 Percilia irwini. Marine and Freshwater Behavior and Physiology 45: 17-28. DOI:
575 10.1080/10236244.2012.668283.
576 Goettel, M. T., Atkinson, J. F., Bennett, S. J., 2015. Behavior of western blacknose dace in
577 a turbulence modified flow field. Ecological Engineering, 74, 230-240.

578 Gross, D., Brevis, W., Jirka, G., 2010. Development of a LED-based PIV/PTV system:
579 Characterization of the flow within a cylinder wall-array in a shallow flow. In: Proc. Int.
580 Conf. on Fluvial Hydraulics River Flow 2010 (pp. 8-10).
581 Habit, E., Dyer, B., Vila, I., 2006. Estado de conocimiento de los peces dulceacuícolas de
582 Chile: estado de su conocimiento. Gayana 70(1), 100-112.
583 Hunter, J. R., Zweifel, J. R., 1971. Swimming speed, tail beat frequency, tail beat
584 amplitude, and size in jack mackerel, trachurus-symmetricus, and other fishes. Fishery
585 Bulletin of the National Oceanic and Atmospheric Administration, 69(2), 253.
586 Jobling, M., 1982. Some observations on the effects of feeding frequency on the food
587 intake and growth of plaice, Pleuronectes platessa L. Journal of Fish Biology, 20(4),
588 431-444.
589 Katopodis, C., Williams, J. G., 2012. The development of fish passage research in a
590 historical context. Ecological Engineering, 48, 8-18.
591 Laborde, A., González, A., Sanhueza, C., Arriagada, P., Wilkes, M., Habit, E. Link, O.,
592 2016. Hydropower development, riverine connectivity and nonsport fish species:
593 Criteria for hydraulic design of fishways. River Research and Applications, 32(9), 1949-
594 1957.
595 Lacey, R. W., Neary, V. S., Liao, J. C., Enders, E. C., Tritico, H. M., 2012. The IPOS
596 framework: linking fish swimming performance in altered flows from laboratory
597 experiments to rivers. River Research and Applications, 28(4), 429-443. DOI:
598 0.1002/rra.1584.

599 Liao, J. C., 2007. A review of fish swimming mechanics and behavior in altered flows.
600 Philosophical Transactions of the Royal Society 362: 1973-1993. DOI:
601 10.1098/rstb.2007.2082.
602 Liao, J. C., Beal, D. N., Lauder, G. V., Triantafyllou, M. S., 2003a. The Kármán gait: novel
603 body kinematics of rainbow trout swimming in a vortex street. Journal of Experimental
604 Biology, 206(6), 1059-1073.
605 Liao, J. C., Beal, D. N., Lauder, G. V., Triantafyllou, M. S., 2003b. Fish exploiting vortices
606 decrease muscle activity. Science, 302(5650), 1566-1569.
607 Link, O., Habit, E., 2015. Requirements and boundary conditions for fish passes of non-
608 sport fish species based on Chilean experiences. Reviews in Environmental Science and
609 Bio/Technology, 14(1), 9-21.
610 Lupandin, A. I., 2005. Effect of flow turbulence on swimming speed of fish. Biology
611 Bulletin, 32(5), 461-466.
612 Maia, A., Sheltzer, A. P., Tytell, E. D., 2015. Streamwise vortices destabilize swimming
613 bluegill sunfish (Lepomis macrochirus). The Journal of Experimental Biology, 218(5),
614 786-792.
615 Melling, A., 1997. Tracer particles and seeding for particle image velocimetry.
616 Measurement Science and Technology, 8(12), 1406.
617 Mitchell, C. P., 1989. Swimming performances of some native freshwater fishes. New
618 Zealand Journal of Marine and Freshwater Research 23: 181-187.
619 Montoya, G., Jara A., Solis-Lufí K., Colin N., Habit E., 2012. Primeros estadíos del ciclo
620 de vida de peces nativos del río San Pedro (cuenca del río Valdivia, Chile). Gayana
621 76(1), 86-100.

622 Nikora, V. I., Aberle, J., Biggs, B. J., Jowett, I. G., Sykes, J. R., 2003. Effects of fish size,
623 time-to-fatigue and turbulence on swimming performance: a case study of Galaxias
624 maculatus. Journal of Fish Biology, 63(6), 1365-1382.
625 Noonan, M. J., Grant, J. W. Jackson, C. D., 2012. A quantitative assessment of fish passage
626 efficiency. Fish and Fisheries, 13(4), 450-464.
627 Oufiero, C. E., Jugo, K., Garland, T., 2014. Swimming with a sword: tail beat kinematics in
628 relation to sword length in Xiphophorus. Functional Ecology, 28(4), 924-932.
629 Pavlov, D. S., Lupandin, A. I., Skorobogatov, M. A., 2000. The effects of flow turbulence
630 on the behavior and distribution of fish. J. Ichthyol., 40(2), 232–261.
631 Piedra, P., Habit, E., Oyanedel, A., Colin, N., Solis-Lufí, K., González, J., Jara, A., Ortiz,
632 N., Cifuentes, R., 2012. Patrones de desplazamiento de peces nativos en el río San Pedro
633 (cuenca del río Valdivia, Chile). Gayana, 76(1), 59-70.
634 Plew, D. R., Nikora, V. I., Larned, S. T., Sykes, J. R., Cooper, G. G., 2007. Fish swimming
635 speed variability at constant flow: Galaxias maculatus. New Zealand Journal of Marine
636 and Freshwater Research, 41(2), 185-195.
637 Ruiz, V.H., 1993. Ictiofauna del río Andalién (Concepción, Chile). Gayana Zoología, 57(2),
638 109-278.
639 Russon, I. J., Kemp, P. S., 2011. Advancing provision of multi-species fish passage:
640 behaviour of adult European eel (Anguilla anguilla) and brown trout (Salmo trutta) in
641 response to accelerating flow. Ecological Engineering, 37(12), 2018-2024.
642 Scarano, F., 2001. Iterative image deformation methods in PIV. Measurement Science and
643 Technology, 13(1), R1.

644 Sfakiotakis, M., Lane, D.M. and Davies, J.B.C., 1999. Review of fish swimming modes for
645 aquatic locomotion. IEEE Journal of oceanic engineering, 24(2), 237-252.
646 Sobenes, C., García, A., Habit, E., Link, O., 2012. Mantención de Peces Nativos
647 Dulceacuícolas de Chile en cautiverio: un aporte a su conservación ex situ. Boletín de
648 Biodiversidad de Chile, 7, 27-41.
649 Taguchi, M., Liao, J. C., 2011. Rainbow trout consume less oxygen in turbulence: the
650 energetics of swimming behaviors at different speeds. The Journal of Experimental
651 Biology, 214(9), 1428-1436.
652 Taylor, G.I., 1935. Statistical theory of turbulence. Proceedings of the Royal Society of
653 London, Series A, 151, 421–444.
654 Thielicke, W., Stamhuis, E. J., 2014a. PIVlab – Towards User-friendly, Affordable and
655 Accurate Digital Particle Image Velocimetry in MATLAB. Journal of Open Research
656 Software 2(1):e30, DOI: http://dx.doi.org/10.5334/jors.bl
657 Thielicke, W., Stamhuis, E. J., 2014b. PIVlab - Time-Resolved Digital Particle Image
658 Velocimetry Tool for MATLAB (version: 1.41).
659 http://dx.doi.org/10.6084/m9.figshare.1092508
660 Triantafyllou, G. S., Triantafyllou, M. S., Grosenbaugh, M. A., 1993. Optimal thrust
661 development in oscillating foils with application to fish propulsion. Journal of Fluids and
662 Structures, 7(2), 205-224.
663 Tritico, H. M., Cotel, A. J., 2010. The effects of turbulent eddies on the stability and critical
664 swimming speed of creek chub (Semotilus atromaculatus).The Journal of Experimental
665 Biology, 213(13), 2284-2293.

Véliz, D., Catalán, L., Pardo, R., Acuña, P., Díaz, A., Poulin, E., Vila, I., 2012. El género Basilichthys (Teleostei: Atherinopsidae) analizado a lo largo de su distribución en Chile (21° a 40° S), utilizando rasgos morfológicos y variabilidad del ADN mitocondrial. Revista Chilena de Historia Natural, 85(1), 49-59.

Victoriano, P., Vera, I., Olmos, V., Dib, M., Insunza, B., Muñoz-Ramírez, C., Montoya, R., Jara, A., Habit, E., 2012. Patrones idiosincráticos de diversidad genética de peces nativos del río San Pedro (cuenca del río Valdivia), un sistema de la región glaciada del sur de Chile. Gayana, 76(1), 71 – 85.

Videler, J. J., 1993. Fish swimming (Vol. 10). Springer Science & Business Media.

Videler, J. J., Wardle, C. S., 1991. Fish swimming stride by stride: speed limits and endurance. Reviews in Fish Biology and Fisheries, 1(1), 23-40. DOI: 10.1007/BF00042660.

Vila, I., Habit, E., 2015. Current situation of the fish fauna in the Mediterranean region of Andean river systems in Chile. Fishes in Mediterranean Environments 2015(2), 1-19.

Vila, I., Soto, D., Bahamondes, I., 1981. Age and growth of Basilichthys australis (Eigenmann 1927) in Rapel reservoir, Chile. Studies on Neotropical Fauna and Environment, 16, 9-22.

Wardle, C., Videler, J. and Altringham, J., 1995. Tuning in to fish swimming waves: body form, swimming mode and muscle function. Journal of experimental Biology, 198(8), 1629-1636.

Webb, P.W., 1971. The swimming energetics of trout. II. Oxygen consumption and swimming efficiency. Journal of Experimental Biology, 55, 521-540.

Webb, P. W., Weihs, D. (Eds.), 1983. Fish biomechanics. Praeger Publishers.

689 Welch, P. D., 1967. The use of fast Fourier transform for the estimation of power spectra:
690 A method based on time averaging over short, modified periodograms. IEEE
691 Transactions on Audio and Electroacoustics, 15(2), 70-73.
692 Westerweel, J., Scarano, F., 2005. Universal outlier detection for PIV data. Experiments in
693 Fluids, 39(6), 1096-1100.
694 Wilkes, M. A., Maddock, I., Visser, F., Acreman, M. C., 2013. Incorporating
695 Hydrodynamics into Ecohydraulics: The Role of Turbulence in the Swimming
696 Performance and Habitat Selection of Stream-Dwelling Fish. In: Ecohydraulics: An
697 Integrated Approach. Wiley, Chichester, 7-30.
698 Williamson, C. H., 1996. Vortex dynamics in the cylinder wake. Annual Review of Fluid
699 Mechanics, 28(1), 477-539.
700 Wu, G., Yang, Y., Zeng, L., 2007. Kinematics, hydrodynamics and energetic advantages of
701 burst-and-coast swimming of koi carps (Cyprinus carpio koi).Journal of Experimental
702 Biology, 210(12), 2181-2191.
703 Zarfl, C., Lumsdon, A. E., Berlekamp, J., Tydecks, L., Tockner, K., 2015. A global boom
704 in hydropower dam construction. Aquatic Sciences, 77(1), 161-170. DOI:
705 10.1007/s00027-014-0377-0.
706